

^{51}V NMR study of the spin-gap compound BiCu_2VO_6 : A microscopic probe of magnetic interactions

C. S. Lue,^{1,*} S. C. Chen,¹ C. N. Kuo,¹ and F. C. Chou²¹*Department of Physics, National Cheng Kung University, Tainan 70101, Taiwan*²*Center for Condensed Matter Sciences, National Taiwan University, Taipei 10601, Taiwan*

(Received 20 April 2009; revised manuscript received 5 August 2009; published 25 September 2009)

We report the results of a ^{51}V nuclear-magnetic-resonance (NMR) study on the quasi-one-dimensional compound BiCu_2VO_6 at temperatures between 4 and 300 K. Three ^{51}V NMR resonance lines that are associated with three nonequivalent crystallographic sites have been resolved. For each vanadium site, the temperature-dependent NMR shift exhibits a character of low-dimensional magnetism with a broad maximum. At low temperatures, all NMR shifts and spin-lattice relaxation rates clearly indicate thermally activated behavior, confirming the spin-gap formation in BiCu_2VO_6 . We further analyze the spin shift data based on a proposed spin-ladder scenario with three different types of interactions along the rungs. With this accordance, the spin gaps and the couplings along the rungs of the ladder are properly estimated.

DOI: [10.1103/PhysRevB.80.092407](https://doi.org/10.1103/PhysRevB.80.092407)

PACS number(s): 76.60.-k, 75.10.Pq

The physics of low-dimensional magnetic systems continues to attract attention because of the association with peculiar quantum effects.¹ Strong quantum fluctuations due to low dimensionality may suppress the long-range magnetic ordering, resulting in an opening of a finite spin gap separated from the spin singlet ground state and magnetic excited states.² During the past decades, quantum spin systems such as $\text{Sr}_{14}\text{Cu}_24\text{O}_{41}$, $(\text{VO})_2\text{P}_2\text{O}_7$, $\text{BaCu}_2\text{V}_2\text{O}_8$, and $\text{Cu}_2\text{Sc}_2\text{Ge}_4\text{O}_{13}$ have been discovered to possess spin gaps.³⁻⁷ The spin-gap characteristics have been interpreted in accordance with the strong spin-exchange interactions of particular configurations along the specific low-dimensional pathways in these compounds.

BiCu_2VO_6 , which adopts a monoclinic structure with the space group $P2_1/n$, was synthesized by Radosavljevic *et al.*⁸ The bulk magnetic susceptibility of BiCu_2VO_6 exhibits a broad maximum at around 120 K and decreases rapidly with lowering temperature.⁹ In addition, the result of the heat-capacity measurement has further confirmed no long-range magnetic ordering above 2 K. These features are in reminiscence of spin-gap characteristics for this material. Taking into account the known oxidation states of O^{2-} and Bi^{3+} , the remaining valences are nonmagnetic V^{5+} and magnetic Cu^{2+} ($S=1/2$). Due to the insulating character in BiCu_2VO_6 ,¹⁰ the superexchange interactions of these copper ions mediated by various oxygen atoms would be responsible for the magnetic nature of this compound. Because of the inherent structural complexity, it is rather difficult to identify all pathways for the superexchange interactions. A simple triple-dimer picture based on eight unique Cu–O–Cu bonds was suggested by Masuda *et al.* for the description of the magnetic property of BiCu_2VO_6 .⁹ However, the fitting of the magnetic susceptibility to such an isolated dimer model was found to be less satisfactory and the discrepancy was attributed to the non-negligible interdimer interactions.⁹ While a more recent analysis with considering the interdimer interaction (zJ') can improve the fitting, the extracted interdimer coupling constant is beyond the validity of the mean-field approximation.¹¹ It was thus speculated that a two-leg spin ladder scenario seemed to be more realistic to the under-

standing of the spin-gap nature in BiCu_2VO_6 .

From the atomic positional parameters refined by Radosavljevic *et al.*,⁸ copper atoms have six nonequivalent crystallographic sites in BiCu_2VO_6 , showing two types of coordination environments. There are two sets of copper pairs (Cu1–Cu2 and Cu5–Cu6) reside in a square-pyramidal environment. For the Cu1–Cu2 pair, two oxygen atoms (O7 and O11) provide the channels for the superexchange interaction (J'_1) between Cu1 and Cu2 spins, resulting in a coupled unit along the b direction. Similarly, O13 and O16 are responsible for the interactions along the rungs (J'_3) of the Cu5–Cu6 pair. The remaining Cu3 and Cu4 atoms are coordinated in a distorted octahedron. The coupling between these two coppers (J'_2) is only bridged by one oxygen atom (O15). Since the interactions along the legs are similar, it is suitable to approximate a uniform interaction J along the legs of the ladder. With this respect, a simple approach based on a two-leg spin ladder containing three different types of rungs is proposed here for the realization of the magnetic features in BiCu_2VO_6 . A schematic for the superexchange interactions within the ladder is illustrated in Fig. 1.

In addition, there are three nonequivalent vanadium crystallographic sites, denoted as V1, V2, and V3, respectively. Since these vanadium sites are nonmagnetic, it allows us to probe the magnetic features of Cu^{2+} ions through the transferred hyperfine interaction,¹² a transfer of the magnetic $3d$ spin from the copper ions onto the vanadium $4s$ orbital in the present case of BiCu_2VO_6 . By virtue of crystallographic criteria, probing the V1 site is expected to sense mostly the magnetic nature of Cu1 and Cu2 ions linked by O7. Similarly, the V2 site would mainly reflect the magnetic interactions of Cu5 and Cu6 mediated by O13. For the V3 site, O15 is responsible for the interacting channel for probing the magnetic properties of Cu3 and Cu4. Therefore, with the study of individual vanadium sites, the results can be used to resolve the magnetic characteristics of three rungs within the ladder. Nuclear magnetic resonance (NMR) is a site-selective tool which provides local magnetic information of the specific site. In this investigation, we thus employ an NMR study invoking the NMR shift measurements of all three ^{51}V

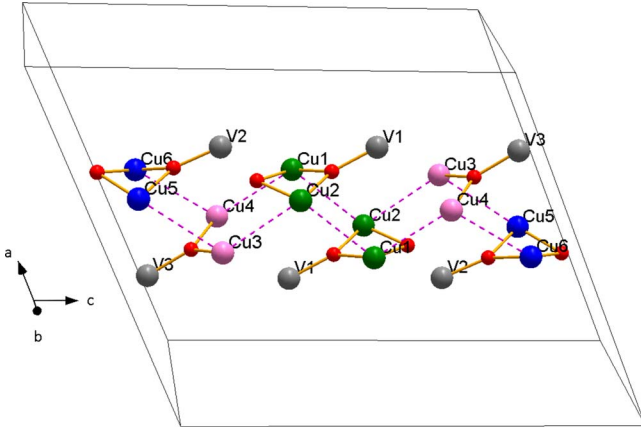


FIG. 1. (Color online) A schematic description of the superexchange interactions in BiCu_2VO_6 . Only atoms involving dominantly magnetic interactions are presented. The dashed lines represent the interaction along the legs of the ladder defined by J .

NMR resonance lines to associate with the magnitudes of the superexchange interactions as well as the spin gaps of BiCu_2VO_6 .

A single-phase BiCu_2VO_6 sample was synthesized by a ceramic sintering solid-state reaction technique described elsewhere.⁸ Briefly, Bi_2O_3 , CuO , and V_2O_5 powders with the stoichiometric ratios were mixed and pressed into pellets. The pellets were sintered at 600 °C for 48 h, and 730 °C for 24 h in air. A brown product was obtained. An x-ray diffraction spectrum taken with $\text{Cu } K\alpha$ radiation on the powder BiCu_2VO_6 specimen was identified within the expected $P2_1/n$ structure with no sign of the presence of other phases.

The dc magnetic susceptibility χ was measured with a superconducting quantum interference device magnetometer (Quantum Design) under an external field of 1 T. The temperature dependence of $\chi(T)$ in the range between 2 and 300 K was given in Fig. 2. The feature of the curve is similar to that reported by Masuda *et al.*,⁹ showing a broad maximum at $T_{max} \approx 125$ K. After passing this maximum, the susceptibility decreases rapidly with lowering temperature, and an upturn appears below 20 K. The susceptibility data can be decomposed into $\chi(T) = \chi_o + \chi_{cw}(T) + \chi_{spin}(T)$ where χ_o is a temperature-independent part, $\chi_{cw}(T) = C/(T - \theta)$ is the Curie-Weiss term responsible for the low-temperature upturn, and $\chi_{spin}(T)$ is the uniform spin susceptibility corresponding to the intrinsic magnetic nature of BiCu_2VO_6 . Based on the low-temperature data fitting to the Curie-Weiss behavior, we obtained the parameters of $\chi_o = 1.3 \times 10^{-4}$ emu/mol, $\theta = -0.96$ K, and $C = 4.110^{-3}$ emu K/mol. From the value of C , the concentration of the paramagnetic defects arising from the isolated Cu^{2+} ions was estimated to be 0.55% per mole in our sample. The spin part can be extracted by utilizing $\chi_{spin}(T) = \chi(T) - \chi_{cw}(T) - \chi_o$, shown as the open triangles in Fig. 2.

For a two-leg Heisenberg spin ladder, the magnetic susceptibility can be well described with an empirical formula proposed by Barnes and Riera as¹³

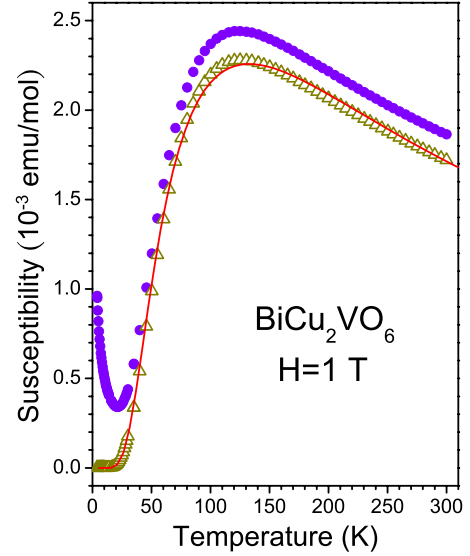


FIG. 2. (Color online) Magnetic susceptibility $\chi(T)$ of BiCu_2VO_6 measured in a field of 1 T (solid circles). The deduced spin part $\chi_{spin}(T)$ is shown as the open triangles. The solid curve corresponds to a fit to the equation of $\chi_{spin}(T)$ described in the text.

$$\chi_{spin}(T) = \frac{c_1}{T} \left[1 + \left(\frac{T}{c_2} \right)^{c_3} (e^{c_4/T} - 1) \right]^{-1} \left[1 + \left(\frac{c_5}{T} \right)^{c_6} \right]^{-1}. \quad (1)$$

Here c_1 is a proportional constant while c_3 and c_6 are exponents which govern the steepness of the low- T drop and the high- T decay, respectively. The factor c_4 is related to the position of the peak, T_{max} , and the parameters c_2 and c_5 are associated with the height of the peak and the high- T magnitude of χ_{spin} , respectively. It should be emphasized that except for c_1 these coefficients are not arbitrary fitting parameters but essentially constrained by the alternation parameter $\alpha \equiv J'/J$. The fitting result is quite satisfactory, shown as a solid curve in Fig. 2. The parameters used for the fit are tabulated in Table I. Since the determined $\alpha \approx 0.98$ is very close to unity, the relationship between the spin gap Δ and J can be expressed as^{13,14}

$$\Delta \approx J[0.5 + 0.65(\alpha - 1)]. \quad (2)$$

The inelastic neutron-scattering experiment has indicated the lowest excitation energy of 16 meV (185 K) which would be

TABLE I. Fitting parameters used for χ_{spin} , $1/T_1$, and each K_{spin} in BiCu_2VO_6 .

	c_1	c_2 (K)	c_3	c_4 (K)	c_5 (K)	c_6
χ_{spin}	0.84	860	0.90	175	120	1.51
$1/T_1$	496	860	0.90	175	120	1.51
Line <i>a</i>	1.04	790	0.88	215	110	1.50
Line <i>b</i>	1.05	830	0.92	190	120	1.52
Line <i>c</i>	1.03	900	0.98	170	122	1.54

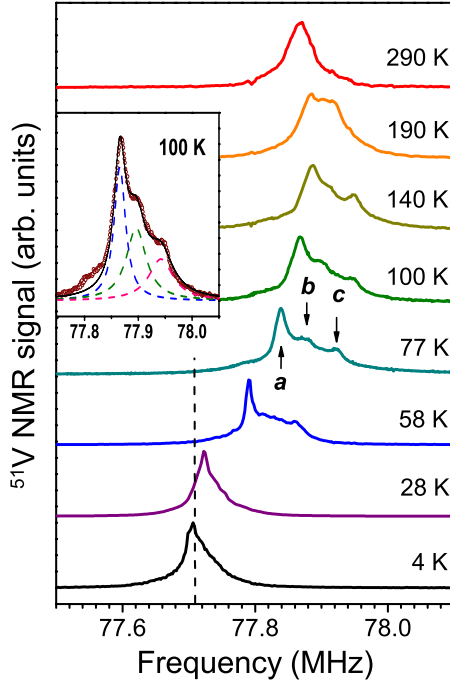


FIG. 3. (Color online) ^{51}V NMR spectra of BiCu_2VO_6 measured at various temperatures under a constant field of 6.9437 T. The dashed vertical line denotes the position of the ^{51}V reference frequency. Inset: a representative plot for the decomposed spectrum measured at 100 K.

the same energy sensed by the magnetic susceptibility.⁹ We thus adopted $\Delta=185$ K to estimate the interacting constant along the legs of the ladder $J=380$ K.

NMR experiments were performed using a Varian 300 spectrometer with a constant field of 6.9437 T. The powder specimen was put in a plastic vial that showed no observable ^{51}V NMR signal. The ^{51}V NMR spectra were obtained by the Fourier transform of a half of the spin-echo signal using a standard $\pi/2-\tau-\pi$ sequence.¹⁵ Since the powder specimen was used, the central transition lines appear as powder patterns, as given in Fig. 3. The spectrum is quite complicated because of the combination of three vanadium resonance lines, denoted as the lines *a*, *b*, and *c*, respectively. To separate these lines, we deconvoluted each individual spectrum into three functions and determined the NMR shift (K_{obs}) of the corresponding resonance line. A representative plot obtained at 100 K was displayed in the inset of Fig. 3. The decomposed K_{obs} 's, referred to the ^{51}V resonance frequency of aqueous VOCl_3 , were shown as a function of temperature in Fig. 4. As one can see, three distinctive curves are resolved. All low-temperature K_{obs} 's exhibit thermally activated behavior and decrease rapidly to almost zero, confirming the presence of a finite-energy gap in the spin-excitation spectrum. However, the steepness of the drops at low temperatures is essentially different among these three curves, implying the existence of multiple spin gaps in this material.

In general, K_{obs} is a combination of two parts as $K_{obs} = K_o + K_{spin}(T)$. The first term K_o is temperature independent while the spin shift K_{spin} , which reflects the Cu^{2+} spin behavior through the transferred hyperfine interaction, is a function

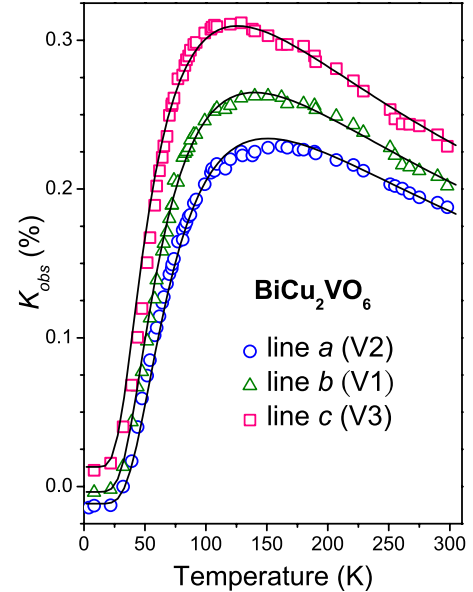


FIG. 4. (Color online) Temperature dependence of the resolved ^{51}V NMR shifts in BiCu_2VO_6 . Solid curves are fits to the spin-ladder model described in the text.

of temperature. As mentioned above, J'_2 is expected to be the weakest interaction among three sets of ladders because the Cu3 and Cu4 ions are bridged by only one oxygen. The corresponding alternation parameter $\alpha_2 \equiv J'_2/J$ should be relative small, leading to a steepest drop of K_{spin} at low temperatures among these three curves. On this basis, it is reasonable to assign the line *c* to the V3 site which probes mostly the magnetic characteristics of Cu3 and Cu4 ions. Similarly, the line *a* would be associated with the V2 site due to the strongest J'_3 produced by Cu5 and Cu6 interactions. The remaining one, line *b*, which appears at the middle of the resonance spectrum is connected to V1.

As in the case of χ_{spin} , each experimental $K_{obs}(T)$ was fitted to Eq. (1) plus K_o and the best-fitting result was displayed as a solid curve in Fig. 4. The parameters used for the fits are also summarized in Table I. From the optimum fit, we can determine the values of J' and α for each individual rung with the results listed in Table II. Since all α values are found to be close to unity, the relation in Eq. (2) is valid for estimating the spin gaps of $\Delta_1=197$ K, $\Delta_2=170$ K, and $\Delta_3=210$ K by substituting the constant $J=380$ K. Comparing to other experimental results, the lowest excitation energy of 185 K observed from the inelastic neutron-scattering experiment⁹ is similar to the gaps extracted from NMR. Although the former exhibits only a single gap, it is possible

TABLE II. Deduced superexchange interactions along the rungs, alternation parameters, and spin gaps in BiCu_2VO_6 .

Rung	J' (K)	α	Δ (K)
Cu1–Cu2	390	1.03	197
Cu3–Cu4	350	0.92	170
Cu5–Cu6	410	1.08	210

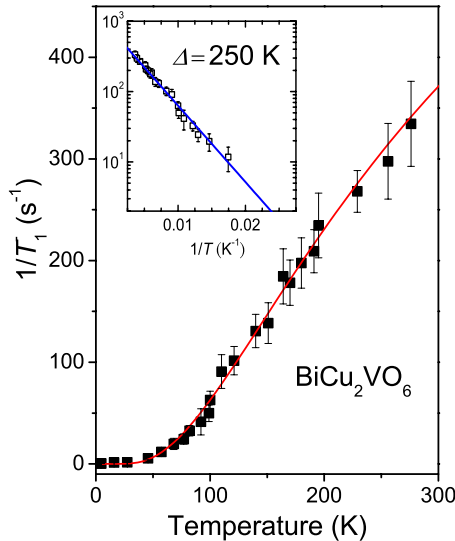


FIG. 5. (Color online) Temperature dependence of the spin-lattice relaxation rate for BiCu_2VO_6 . The solid curve is the fitted function according to Eq. (3). Inset: inverted temperature dependence of $1/T_1$. The solid line is a fit to the activation law $1/T_1 \propto \exp(-\Delta/T)$.

for these to be reconciled if we consider that the very broad excitation peak in the energy dependence of the inelastic neutron-scattering strength is a combination of these three excitation gaps.

To gain more insight into the spin-gap characteristics of BiCu_2VO_6 , we performed the spin-lattice relaxation-rate ($1/T_1$) measurement, being sensitive to the low-energy magnetic excitations. As shown in Fig. 5, the temperature dependence of $1/T_1$ exhibits activated behavior, indicative of the presence of an energy gap in the magnetic excitations. An Arrhenius plot of $1/T_1$ between 50 and 280 K is displayed in the inset of Fig. 5. From the linear relation, we can extract

the spin gap of $\Delta=250$ K. This value is a bit larger than those obtained from the Knight shifts. As a matter of fact, the $1/T_1$ result represents an averaged contribution from three different sites as in the case of χ_{spin} because it is difficult to isolate these resonance lines in the relaxation-rate measurements due to the mergence of these lines at low and high temperatures. Within the low-temperature limit, the local dissipative susceptibility sensed by $1/T_1T$ and the static susceptibility probed by K_{spin} would be almost identical. With this respect, both static and dynamic excitations follow the same temperature variation and $1/T_1$ should be fitted to the form by analogy to the treatment of the NMR shift as

$$\frac{1}{T_1} = c_1 \left[1 + \left(\frac{T}{c_2} \right)^{c_3} (e^{c_4/T} - 1) \right]^{-1} \left[1 + \left(\frac{c_5}{T} \right)^{c_6} \right]^{-1}. \quad (3)$$

Using the same parameters as those in χ_{spin} , the fitting result, drawn as a solid curve in Fig. 5, is very satisfactory, indicating that the present analysis is quite reliable.

In summary, we reported the ^{51}V NMR investigation of BiCu_2VO_6 and analyzed the spin-shift data according to a proposed two-leg spin-ladder scenario with three types of interactions along the rungs. On this basis, we obtained concrete estimates of individual interactions along the rungs as well as the spin gaps. The NMR observations are found to be consistent with the results from the inelastic neutron-scattering experiment. It thus reinforces the conclusion that the proposed interpretation for the NMR shifts and determined couplings are appropriate for the case of BiCu_2VO_6 . Apparently, the existence of multiple gaps in BiCu_2VO_6 is unique among the low-dimensional spin-gap materials and it deserves further experimental and theoretical investigations.

This work was supported by the National Science Council of Taiwan under Grant No. NSC-98-2112-M-006-011-MY3 (CSL).

*cslue@mail.ncku.edu.tw

- ¹P. Lemmens, G. Guntherodt, and C. Gros, Phys. Rep. **375**, 1 (2003) and references therein.
- ²A. N. Vasil'ev, M. M. Markina, and E. A. Popova, Low Temp. Phys. **31**, 203 (2005) and references therein.
- ³K. I. Kumagai, S. Tsuji, M. Kato, and Y. Koike, Phys. Rev. Lett. **78**, 1992 (1997).
- ⁴T. Imai, K. R. Thurber, K. M. Shen, A. W. Hunt, and F. C. Chou, Phys. Rev. Lett. **81**, 220 (1998).
- ⁵J. Kikuchi, K. Motoya, T. Yamauchi, and Y. Ueda, Phys. Rev. B **60**, 6731 (1999).
- ⁶Z. He, T. Kyomen, and M. Itoh, Phys. Rev. B **69**, 220407(R) (2004).
- ⁷C. S. Lue, C. N. Kuo, T. H. Su, and G. J. Redhammer, Phys. Rev.

B **75**, 014426 (2007).

- ⁸I. Radosavljevic, J. S. O. Evans, and A. W. Sleight, J. Solid State Chem. **141**, 149 (1998).
- ⁹T. Masuda, A. Zheludev, H. Kageyama, and A. N. Vasilev, Europhys. Lett. **63**, 757 (2003).
- ¹⁰I. Radosavljević Evans, S. Tao, and J. T. S. Irvine, J. Solid State Chem. **178**, 2927 (2005).
- ¹¹O. Mentre, E. M. Ketatni, M. Colmont, M. Huve, F. Abraham, and V. Petricek, J. Am. Chem. Soc. **128**, 10857 (2006).
- ¹²C. S. Lue and B. X. Xie, Phys. Rev. B **72**, 052409 (2005).
- ¹³T. Barnes and J. Riera, Phys. Rev. B **50**, 6817 (1994).
- ¹⁴T. Barnes, E. Dagotto, J. Riera, and E. S. Swanson, Phys. Rev. B **47**, 3196 (1993).
- ¹⁵C. N. Kuo and C. S. Lue, Phys. Rev. B **78**, 212407 (2008).